Hybrid multi-layered scaffolds produced via grain extrusion and electrospinning for 3D cell culture tests

Paola Ginestra, Stefano Pandini and Elisabetta Ceretti
Department of Mechanical and Industrial Engineering, University of Brescia, Brescia, Italy

Abstract

Purpose – The purpose of this paper is to focus on the production of scaffolds with specific morphology and mechanical behavior to satisfy specific requirements regarding their stiffness, biological interactions and surface structure that can promote cell-cell and cell-matrix interactions though proper porosity, pore size and interconnectivity.

Design/methodology/approach – This case study was focused on the production of multi-layered hybrid scaffolds made of polycaprolactone and consisting in supporting grids obtained by Material Extrusion (ME) alternated with electrospun layers. An open source 3D printer was utilized, with a grain extrusion head that allows the production and distribution of strands on the plate according to the designed geometry. Square grid samples were observed under optical microscope showing a good interconnectivity and spatial distribution of the pores, while scanning electron microscope analysis was used to study the electrospun mats morphology.

Findings – A good adhesion between the ME and electrospinning layers was achieved by compression under specific thermomechanical conditions obtaining a hybrid three-dimensional scaffold. The mechanical performances of the scaffolds have been analyzed by compression tests, and the biological characterization was carried out by seeding two different cells phenotypes on each side of the substrates.

Originality/value – The structure of the multi-layered scaffolds demonstrated to play an important role in promoting cell attachment and proliferation in a 3D culture formation. It is expected that this design will improve the performances of osteochondral scaffolds with a strong influence on the required formation of an interface tissue and structure that need to be rebuilt.

Keywords Material extrusion, Electrospinning, Polycaprolactone, Scaffolds, Fused deposition modeling, Hybrid, Morphology

Paper type Research paper

Introduction

Several techniques have been developed with the aim to produce three-dimensional substrates and scaffolds suitable for tissue engineering, both conventional and non-conventional (Ferraro *et al.*, 2017; Ginestra *et al.*, 2019). One of the main issues in 3D scaffolds fabrication is the need to mimic the extra cellular matrix (ECM) closely enough to allow cells growth and proliferation and to permit the diffusion of nutrients (Sobral *et al.*, 2011; Gastaldi *et al.*, 2015). The electrospinning (ES) process has been held as a highly promising technology for producing nanofibers which mimic the structure of natural ECM (Agarwal *et al.*, 2008). ES normally results in a fibrous randomly-oriented structure, which means it cannot be fully controlled to acquire an ordered morphology and to accurately form the desired microstructure of the scaffold. In addition, the electrospun scaffolds show limited mechanical properties during implantation and tissue regeneration. A limited number of studies reported the possibility to obtain high aligned fibers by the modification of the collector geometry (Li *et al.*, 2003; Li *et al.*, 2004) or the optimization of the melt ES writing process (Wunner *et al.*, 2018). To improve the deficiency of mechanical properties of electrospun fibers, several studies have demonstrated various blending systems, process parameters designs, and post-processing treatments (Inverardi *et al.*, 2018). Furthermore, elctrospinning has been modified or combined with various other fabrication methods (Castells-Sala *et al.*, 2013; Ginestra *et al.*, 2017a; Ginestra *et al.*, 2016). Among different 3D printing methods, material extrusion (ME) technologies have been largely used in the manufacturing of biofunctional scaffolds for tissue engineering. ME has been extensively studied for scaffolds production thanks to the possibility to fabricate porous polymeric substrates with a reproducible structure and customized external and internal morphology (Zein *et al.*, 2002; Domingos *et al.*, 2009). In fact, the final 3D architecture of the scaffold is determined by the pattern of the deposited filament in each single layer (Kundu *et al.*, 2015; Mota *et al.*, 2011). However, the surfaces are usually too smooth and the pore size between the strands is still too large compared to the cell's dimensions. On the other hand, electrospun nano fibrous scaffolds present high surface area, high porosity and interconnected pores of the appropriate size. However, they are not appropriate for fabricating 3D scaffolds because of their poor mechanical properties (Ahn *et al.*, 2012). In this study, with the aim to combine the stiffness and ease of manufacturing of the ME structure with the good tissue

The current issue and full text archive of this journal is available on Emerald Insight at: **www.emeraldinsight.com/1355-2546.htm**

Rapid Prototyping Journal
© Emerald Publishing Limited [ISSN 1355-2546]
[DOI 10.1108/RPJ-03-2019-0079]

Received 22 March 2019
Revised 4 October 2019
Accepted 13 November 2019

engineering capabilities of the electrospuns, a specific hybrid structure was produced (Chen *et al.*, 2009; Dalton *et al.*, 2013). The structure is fabricated through a hybrid method, that combines ME system and ES, and that could be an efficient method for fabricating high quality 3D polymeric scaffolds (Kim *et al.*, 2008; Giannitelli *et al.*, 2015). ME allowed to obtain rigid supporting layers by depositing, with a predefined pattern, an extruded filament of a polymer melt. Afterwards, the 3D scaffold is built by alternating printed layers and webs of nanofibers of polycaprolactone (PCL) to obtain a high-quality scaffold (Liu *et al.*, 2007; Wei and Dong, 2014). Nevertheless, the main issue connected with the combination of the two technologies lies in the interaction between two different states of the material when the same polymer is used in both the production techniques (Park *et al.*, 2008; Lara-Padilla *et al.*, 2017; Moroni *et al.*, 2008). More precisely, the direct printing of the extruded PCL on the top of the electrospun mat causes the total melting of the fibers in correspondence of the adhesion site whereas the ES of the fibers on the top of the ME sample cannot assure a sufficient adhesion of the two layers in preparation of the cell culture (Martins *et al.*, 2009). To overcome these limitations, hybrid 3D scaffolds were prepared by employing a new efficient method to allow the ME and the electrospun layers adhesion to sustain a co-culture cell experiment and still maintaining the inherent layer's morphologies and structure. To strengthen the potential of this method for the production of scaffolds characterized by the same polymer processed with different technologies, the different types of hybrid scaffolds featuring a different structure of the ME layers have been compared in terms of their mechanical properties. The biological outcome of both ME and hybrid scaffolds has also been evaluated. In particular, dynamic culture tests have been performed in a bioreactor allowing a 3D cell culture. Human osteoblasts and equine chondrocytes were seeded on the two sides of the hybrid scaffolds to obtain a co-culture in which the two phenotypes can communicate through the electrospun layers without migrating on the other side of the scaffolds.

Materials and methods

In this section, the production process leading to the obtainment and characterization of the hybrid scaffolds is reported. Poly(ε-caprolactone) grains (45,000 g/mol, Sigma Aldrich) are firstly electrospun into nanofibers and then extruded to produce ME square grids with different pore sides, following previously optimized processes (Ginestra *et al.*, 2017a; Ceretti *et al.*, 2017). Both the electrospun and extruded layers' mechanical properties are therefore analyzed. Thus, the electrospun and ME layers are combined to obtain the hybrid structures that are going to be mechanically and biologically tested. Three replicas of each produced substrate have been analyzed for the tests described below.

Electrospinning tests

Polycaprolactone was dissolved in Glacial Formic Acid (GFA). The solutions were prepared as described in (Ginestra *et al.*, 2017a). Briefly, a solution of 35 per cent of concentration of PCL was poured into a 10 ml syringe, equipped with 21 G needle. The flow rate of the solution was set to be 0.1 ml/h (Fresenius Kabi Injectomat Agilia syringe pump) and a voltage of 20 kV was applied (Gamma High Voltage ES20P-5W power supply). The deposition distance was measured from the needle tip to the grounded collector top and set at 50 mm. Tests were run for 5 min each and then the samples were observed by scanning electron microscope (SEM). The tests were repeated three times under the same conditions to check the system variability based on the diameters of the fibers deposited on the collector.

ME tests

This study was focused on producing scaffolds with the Fab@home 3D printer (Figure 1), using a grains extrusion head, that is able to melt the PCL grains at a fixed temperature of 80°C allowing filaments formation and distribution on the plate according to the designed trajectory (Ceretti *et al.*, 2017).

The head movement in XY axes directions was changed to define the dimension of the pores (in terms of the square side length) while the vertical movement (z-axis) of the head between the depositions of each layer was fixed (Path Height) to assure a proper deposition of the filament on consecutives layers. Table I illustrates the combination of parameters used in the ME samples production:

Hybrid scaffolds

The hybrid scaffolds have been obtained by the adhesion between the electrospun mats and the ME samples. The ME samples with four layers were chosen to be combined with the electrospun layers and produce the hybrid scaffolds. In this way, a proper comparison between the ME samples with 8 layers and the hybrid scaffolds can be performed. The central portion of the electrospun deposition area was removed from the collector and cut to form square specimens with an overall length of 10 mm. In particular, the ME with four layers/electrospun PCL/ME with 4 layers' structures were joined together by the application of a moderate force (4 N) at the onset of the PCL melting (58°C). This was performed by

Figure 1 The Fab@home extruder machine

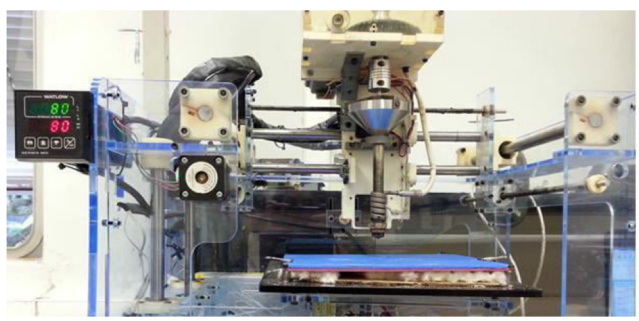

Table I Summary of the process parameters used with the fab@home printer

Layers #	Path Height (PH) (mm)	Pore Side (PS) (mm)
4	0.3	0.3-0.4-0.6-0.8-1
8	0.3	0.3-0.4-0.6-0.8-1

means of a Dynamic-Mechanical Analyzer (DMA Q800 - TA INSTRUMENTS) and the samples were left to cool down in the freezer for about 10 min afterwards.

Mechanical tests

To determine the ability of scaffolds to stand compressive loads via the generation of tensile loads, the mechanical response of the electrospun layers was evaluated in cyclic loading-unloading tests carried out at 23°C by means of a Dynamic-Mechanical Analyzer while the ME and hybrid systems were subjected to compression tests, carried out at 23°C by means of the Instron 366 electromechanical dynamometer.

Cyclic loading-unloading tests

The tensile properties of the electrospun PCL (dissolved in GFA) have been previously analyzed (Ginestra *et al.*, 2017b). To evaluate the possibility to undergo cyclic deformation history, electrospun specimens were subjected to tensile loading-unloading tests. The cyclic tests were performed under tensile conditions by means of a Dynamic-Mechanical Analyzer (DMA Q800 - TA INSTRUMENTS) on strips cut from the central portion of the mat according to the following geometry: overall length of 30 mm and average thickness of 0.5 mm and average width of 10 mm. The equivalent area of interest (10×10 mm^2) was considered the central part of the specimen. A nominal value of stress for the electrospun material was evaluated as the force normalized over the specimen cross-section (about 10×0.5 mm), in order to properly compare the response of specimens that may present, due to their production, different width and thickness. Load-controlled conditions were adopted, and the specimens were subjected to a cyclic deformation between a maximum and minimum level of stress for 60 cycles. Three different levels of maximum stress were explored (1.9 MPa; 2.5 MPa; 3.0 MPa), while a minimum value of force equal to 0.05 N (corresponding to about 0.08 MPa) was set in order to avoid lack of load control at the end of unloading due to specimen buckling. The three tests were carried out at different loading rates (absolute values: 4.5 N/mm; 7 N/mm; 12 N/mm), increasing with the maximum level of load, so to provide a uniform duration of all the tests (i.e. 60 min).

Compression tests on material extrusion samples

Three specimens with a square section, a width of about 10 mm and a thickness depending on the structure of the specific material set were considered. The thickness ranged between about 1.45-1.7 mm in the case of the samples formed by 4 deposited layers and of about 2.4-2.7 (i.e. almost the double) mm in the case of the samples formed by 8 layers. The specimens were subjected to a compressive ramp under displacement control at 1 mm/min up to large strain values (maximum compression strain always above 0.5 mm/mm).

The following ME were tested:

- ME with 4 deposited layers;
- ME with 8 deposited layers; and
- Hybrid scaffolds formed by ME with four deposited layers and eletrospun layers.

The results are reported as compression stress vs. compression strain curves, where compression stress is the stress normalized on the overall specimen cross-section (about 10×10 mm), while compression strain is the crosshead strain normalized on the overall specimen thickness. This representation although dealing with stress and strain values closely related to the ME degree of porosity, was conveniently chosen since allowed an easier comparison of the various hybrid structures, avoiding effects ascribed to differences in the hybrid samples' cross-section.

Biological tests

A co-culture was chosen for the cell culture tests on the hybrid 3D scaffolds with a ME pore side of 0.6 mm and the ME scaffolds with 8 layers and a pore side of 0.6 mm. In particular, the tests performed on the hybrid scaffolds were carried out by means of a static initial culture followed by a 3D culture in a bioreactor chamber connected to the Ismatec® IP High Precision Multichannel Pump while the ME samples were subjected only to the initial static culture test. Human primary osteoblasts (BS PRC 66) were seeded on one side of the scaffolds and equine primary chondrocytes (culture of the Zooprophylactic institute of Lombardy and Emilia-Romagna region) on the other. Cultures were trypsinized, resuspended as single cells and seeded at a cellular density of 20,000 cells/cm^2. Concentrated cell suspension was deposited onto each scaffold and incubated for 45 min before filling the culture dish with a proper volume of culture medium. The cells were cultured using Dulbecco's modified Eagle's medium supplemented with 10 per cent fetal bovine serum, 100 IU/ml penicillin, 100 μg/ml streptomycin and 2 mM L-glutamine. All cell culture reagents were purchased from Thermo Fisher Scientific. Cells were maintained at 37°C in a saturated humidity atmosphere containing 95 per cent air and 5 per cent CO_2. Before cell seeding, all the scaffolds were firstly washed in ethanol (90 per cent) and then in PBS three times for 10 min. The samples were also sterilized under UV light. After four days of static culture, the hybrid scaffolds were moved into the bioreactor chamber with controlled culture medium flow rate of 0.5 ml/h (Figure 2). The samples were tested using optic microscope images for cell static culture highlighting the full recognition of the PCL electrospun surface in terms of cellular adhesion and spreading.

Fluorescent images were generated to evaluate the results of the dynamic culture tests. The immunofluorescence staining was carried out with anti-tubulin antibody to recognize the cells cytoskeletal component. In particular, in order to verify that the ES layer kept the different kinds of cultured cells separated, a human specific antibody, which do not recognize equine cells, has been used. After five days, the scaffolds were fixed for 30 min using Fix&Perm Sample Kit (15 min fixation and 15 min permeabilization), incubated for 45 min with blocking solution (iBindTM 5X Buffer Invitrogen), and stained for 1 hour at room temperature with Monoclonal Anti-Tubulin antibody (T5168 Sigma-Aldrich) diluted 1:200 in the blocking solution. After primary antibody incubation, scaffolds have been washed three times in PBS for 10 min. The scaffolds

Figure 2 Example of Hybrid scaffolds in the bioreactor chambers (1 and 2) connected to the multichannel pump (3), the speed is set at 35 rpm and the reserve (4) is filled of 20 ml of the culture medium that is feeding both the chambers

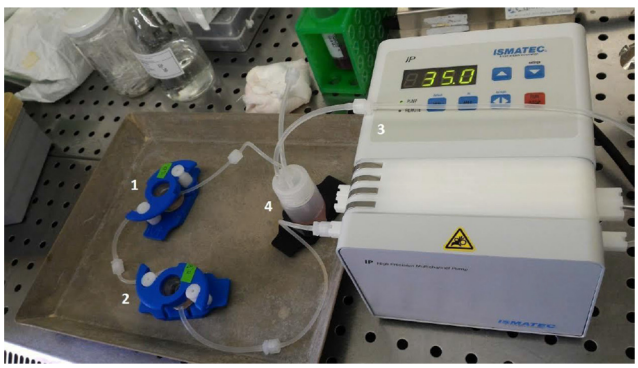

were then incubated for 1 hour at room temperature in the dark with the secondary antibody conjugated with Alexa Fluor® 488 (Thermo Fisher Scientific) diluted 1:250 in the blocking solution. Finally, the scaffolds were stained with Hoechst 33342 diluted 1:100 in PBS for 5 min to highlight the cellular nuclei.

Results

Fibers diameter

The fiber diameter measurements were obtained by using the program ImageJ (Rasband, 2011). Every image was divided into smaller sections, to make a total of at least 60 acquired measurements. SEM analysis results are reported in Figure 3 for three of the electrospun mats.

A randomly oriented nonwoven fiber structure is shown. Table II illustrates the average fiber diameter (AD) and the standard deviation (SD) resulting from the ES tests.

As reported in (Park *et al.*, 2008), the uniformity of the electrospun fibers plays a crucial role in determining the repeatability of the experimental conditions. The standard deviation of the fiber's diameter founded in each sample is demonstrating that the process can be considered stable during the deposition of this polymer solution (Table II). Moreover, the variation between the average diameter calculated for each repetition of the sample indicates that the resulting fibrous mat morphology is strongly dependent on the process parameters. Therefore, the produced electrospun layers with the selected process parameters have be used for the fabrication of the hybrid scaffolds.

Table II Summary of the fiber diameter measurements [average diameter (AD) and standard deviation (SD)] for each repetition

Fiber mat	AD (μm)	SD (μm)
1	0.246	0.040
2	0.210	0.037
3	0.240	0.038

ME square models

The printed layers are characterized by different pores dimension (between 0,3 and 1 mm), layers number (4 and 8) and a path height of 0,3 mm. The images of Figure 4 show the differences between some representative scaffolds produced:

The samples with 4 layers have been analyzed to understand the reproducibility and repeatability of the process (Lara-Padilla *et al.*, 2017). Briefly, the diameter of the filaments and the pore sides were measured and statistically analyzed using ANOVA in order to identify the process parameters that significantly affect the dimensions and the precision of the ME scaffolds (p-value ≤ 0.5). The analysis of the dispersion of the data concluded that the grains extrusion head assures the process stability during the extrusion of this polymer by maintaining the uniformity of the filament diameter during the extrusion process.

Hybrid scaffolds

Figure 5 shows the SEM images of the hybrid scaffolds after the adhesion of the ME and electrospun layers and how the electrospun fibers are not damaged by the adhesion process as the partial melting of the mat is located only at the interface with the ME layer. The hybrid scaffolds were put into a refrigerator at a temperature of 4°C for other ten min. The obtained specimens were then featuring the different pore sizes of the ME samples alternated with electrospun layers.

Mechanical cyclic loading tests

The material behavior of the electrospun layers under the three maximum levels of stress is reported in terms of loading-unloading curves [Figure 6(a)], strain evolution as a function of time [Figure 6(b)], and strain amplitude ($\Delta\varepsilon = \varepsilon_{max} - \varepsilon_{min}$) measured at each cycle [Figure 6(c)]. Stress and strain values were calculated as engineering values from the values of force (F) and displacement (ΔL) recorded during the tests.

The stress vs strain curves clearly show that under all the maximum stress level conditions the materials undergo mechanical hysteresis, which is accompanied by a progressive shift of the cycle towards higher levels of strain. As expected, the effect is moderate, but still present for stress below the knee

Figure 3 Electrospun mats obtained with the selected process parameters: the image shows three repetition of the same test

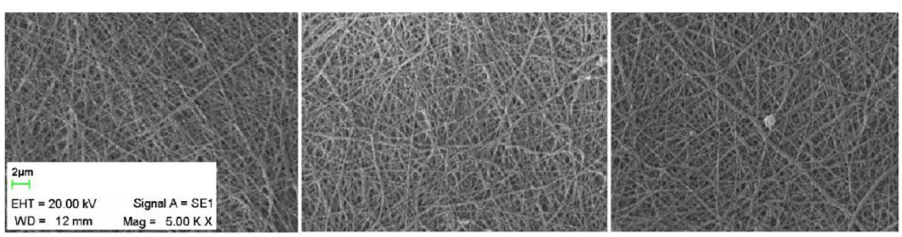

Figure 4 Image of scaffold by ME with PH = 0,3mm

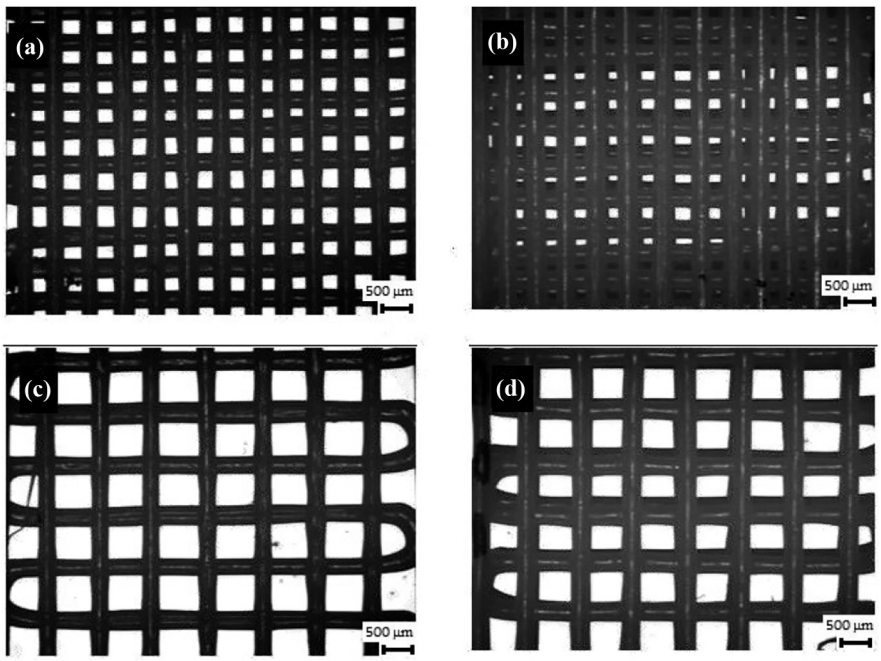

Notes: (a) PS = 0,3mm, NL = 4; (b) PS = 0,3mm, NL = 8; (c) PS = 0,8mm, NL = 4; (d) PS = 0,8mm, NL = 8

Figure 5 SEM images at different magnification of the hybrid scaffolds after the adhesion process

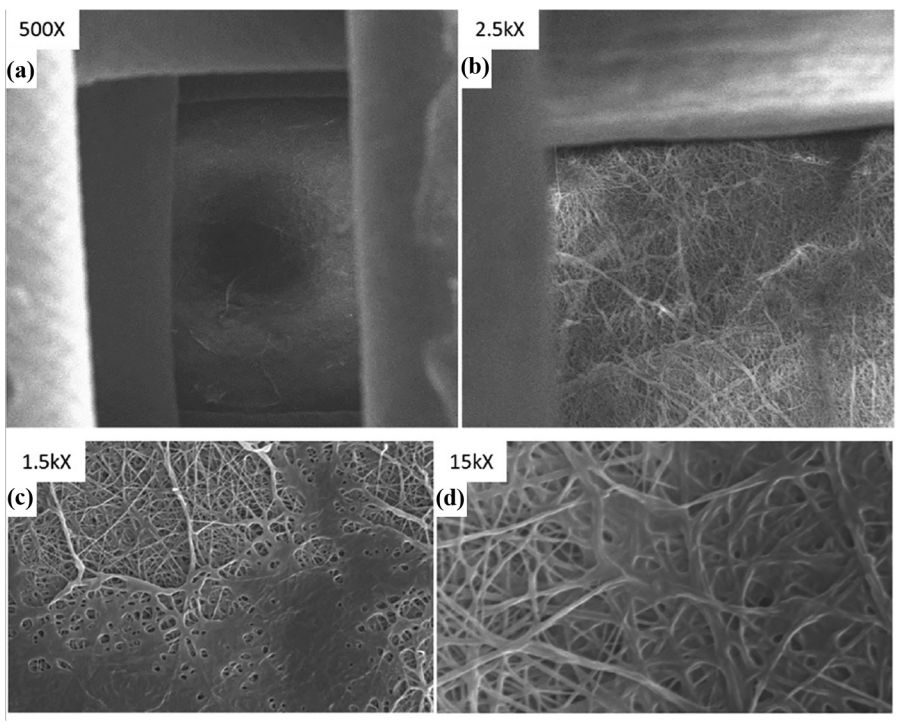

Notes: The scaffold from the top view (a, 500X) and the detail on the proximity of the two samples (b, 2.50kX). SEM images at different magnification of the electrospun sample when the ME sample is forcedly removed after the thermal adhesion: it can be noticed that the adhesion process causes only a limited melting of the top fibers (c) that is restricted to the interface area (d)

Figure 6 (a) Cyclic stress vs strain curves for the electrospun PCL subjected to loading-unloading tests at various maximum load levels (σ_{max} = 1.7 MPa, 2.5 MPa, 3 MPa), where the black curves represent the 30th and 60th cycle; (b) strain evolution as a function of time for the various maximum load levels; (c) cyclic strain variations, $\Delta\varepsilon$, as a function of cycles for the various maximum load levels

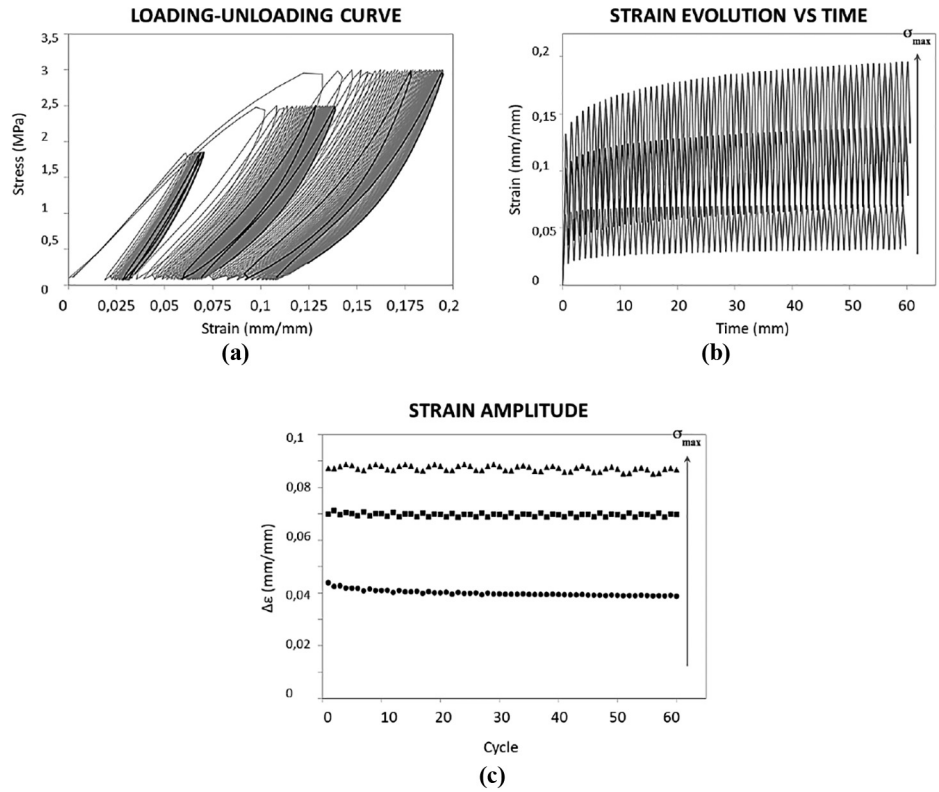

point, and it increases with the maximum level of stress. The continuous shift of the strain to higher values does not attain a proper steady state during the 60 cycles for all the loading conditions, but only for the lowest level of maximum stress, while it seems to approach a steady state value for a higher number of cycles as the maximum stress increases. Interestingly, the shape of the hysteresis cycle and the overall strain variation within the cycle remains practically constant as the number of cycles increases. These results show that by a proper adoption of the maximum stress it is possible to obtain a predictable and constant strain variation, $\Delta\varepsilon$, and that a preliminary cyclic mechanical history, requiring longer times as the maximum load increases, may be helpful in stabilizing the average strain level.

Mechanical compression tests

The compression tests results, reported in terms of the compression stress (i.e. stress over the overall section) vs the compression strain (i.e. the strain over the overall specimen thickness), were analyzed and compared in Figure 7(a) and (b), as the most representative apparent stress vs apparent strain curve for each material group. In such a representation, the employ of compression stress/strain is justified in order to compare specimen with different cross section and thickness: in fact, the structure of the ME samples cannot be uniform from one sample to another. The stress vs. strain curve stiffness (i.e. the slope of the curve in the linear initial trend) is reported and the value of the compression stress at a strain equal to 60 per cent ($\sigma_{60\%}$), was arbitrarily chosen as representative of a highly compression state of the ME samples. The hybrid scaffolds were subjected to the same compression tests as described for the ME samples [Figure 7(c)]. The thickness ranged between about 2.6 and 3.5 mm. The difference between the thickness of the hybrid and the ME samples with 8 layers is probably due to the compression stress applied to achieve adhesion between ME and electrospun layers for the production of the hybrid scaffolds and suggests that the adhesion process led to a certain compaction of the ME in the hybrid arrangement. The data obtained from the compression tests are reported in Table III.

All the curves show the occurrence of a three stage compression history, as suggested by the three different slopes of the curves: the early deformation of the structure allows to evaluate the material stiffness at small strain; this trend is followed by a reduction of the slope as a probable consequence of the collapse of the ME structure trough local flexure of the ME wires, occurring for both system at a compression strain of about 0.1; finally, a subsequent increase of the slope is found after the collapsed structure has approached a more compact state. The curves show a very similar response for both ME and hybrid systems, with very similar values of stiffness and only slight differences in case of the stress at 60 per cent for the two ME systems with a same pore side. As expected, a decrease of the system overall stiffness is found as the pore side increases, and similar decreasing trend is found independently on the

Figure 7 Compression stress vs. strain curves obtained from the compression tests performed on the ME samples with 4 (a), 8 (b) extruded layers and on the hybrid scaffolds (c), Stiffness versus pore side average value (d)

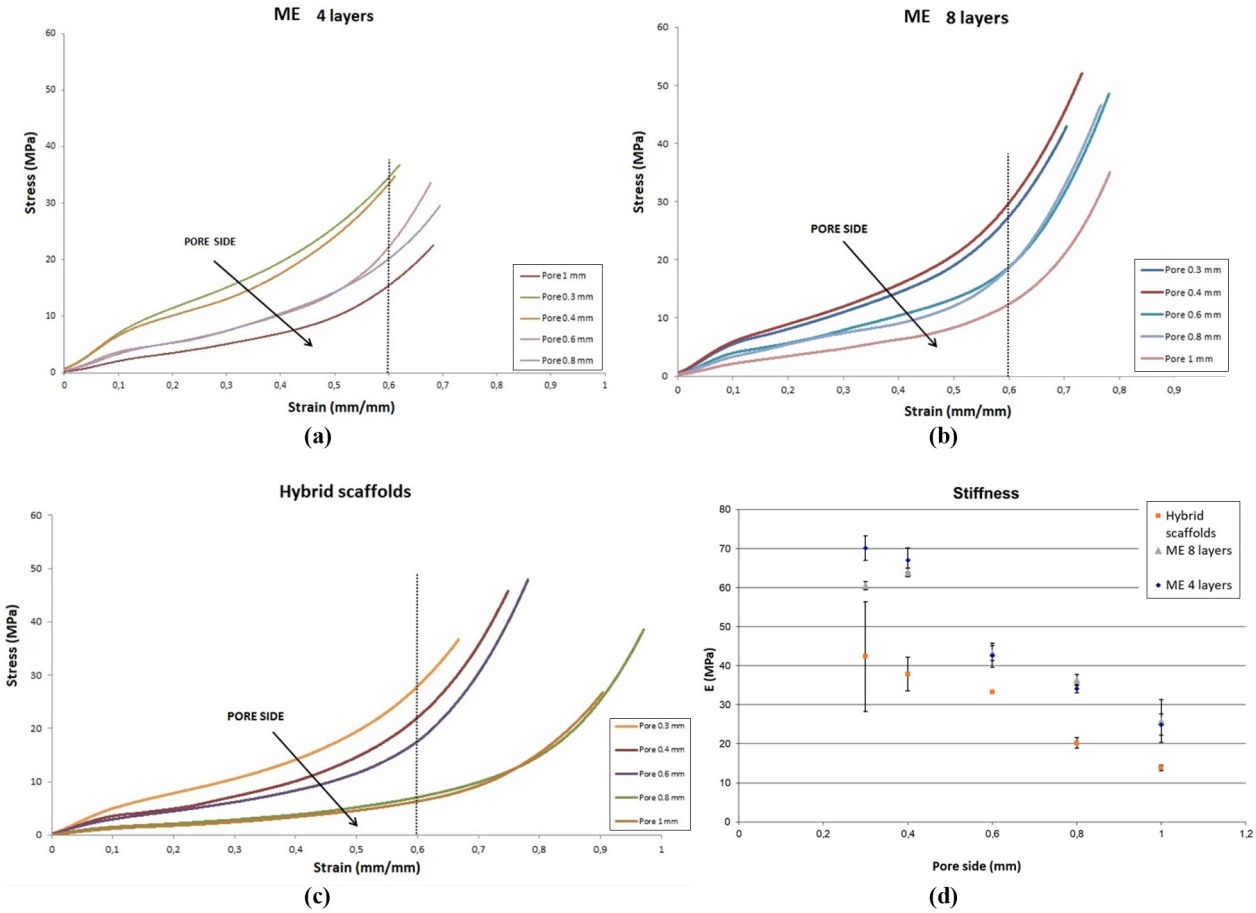

Note: It is worth to remark that compression stress refers to a value normalized on the overall specimen cross-section, and compression strain to a value normalized on the overall specimen thickness

Table III Stiffness (E) and normalized force at a strain equal to 60% for the samples tested under compression

Layers #	PS (mm)	E (MPa)	$\sigma_{60\%}$ (MPa)
4	0.3	70 ± 3*	35 ± 1*
4	0.4	67 ± 3*	32 ± 0.8*
4	0.6	42 ± 3*	22 ± 0.6*
4	0.8	34 ± 1*	20 ± 0.2*
4	1	20 ± 2*	17 ± 3*
8	0.3	60 ± 1*	27 ± 0.6*
8	0.4	63 ± 1*	29 ± 0.2*
8	0.6	43 ± 1*	19 ± 0.5*
8	0.8	36 ± 1*	18 ± 0.2*
8	1	25 ± 5*	14 ± 3*
Hybrid 1	0.3	42 ± 14*#	21 ± 8*#
Hybrid 2	0.4	37 ± 4*#	19 ± 3*#
Hybrid 3	0.6	33 ± 2*#	17 ± 0.2*#
Hybrid 4	0.8	20 ± 1*#	7 ± 0.5*#
Hybrid 5	1	13 ± 0.7*#	6 ± 1*#

Note: where * signifies p-value < 0.05 (# Box-Cox transformation)

number of the layers of the ME samples [Figure 7(d)]. This suggests the possibility to easily tune the stiffness of the structure, and to vary the object structure without significant changes in the overall stiffness. From the compact samples (pore side ≤ 0.6 mm) it is more evident the presence of an early elastic deformation stage corresponding to a compression up to a level of strain equal to 10 per cent, a subsequent collapse stage up to a strain equal to 40-50 per cent of compression followed by a final hardening stage. The stress at 60 per cent of compression is influenced by the number of the layers of the ME samples due to an effect of densification of the structure that requires higher levels of stress for the samples consisting of 4 layers with respect to those obtained through 8 deposited layers. The hybrid scaffolds showed a peculiar mechanical response due the change of structure caused by the adhesion process between the ME samples and the ES layer as seen by comparing the mechanical performances of the hybrid scaffolds with respect to the ME samples. In particular, a lower stiffness of the hybrid samples compared to the ME samples with the same number of layers (8) is found and also the collapse stage of the samples is occurring at lower levels of stresses compared

to the ME samples resulting in a softer material with tailored mechanical properties due to the final geometry of the hybrid structure.

Cell culture tests

The optical microscope images are showing the difference in terms of cellular adhesion on the samples due to the presence or the absence of the ES layer between the ME layers. The optical images were taken after four days of static culture. In particular, as shown by Figure 8, if the cells are seeded on the ME samples (8 layers), it is possible to observe the formation of an ECM layer on the hydrophobic surface of the PCL filaments resulting in an only partial colonization of the structure. As a matter of facts, the cells are not easily visible on the filaments as the majority of them remains attached on the bottom of the sample holder.

On the other hand, as shown in Figure 9, the cellular colonization seems to be highly promoted by the presence of the ES layer due to its surface morphology that is promoting the cellular attachment and spreading on the entire hybrid structure. In this case, the number of the cells founded on the filaments is strongly increased due to the containment effect caused by the ES layer.

Immunofluorescence staining

The hybrid scaffolds were mounted onto glass slides and observed with an inverted fluorescent microscope. As shown by fluorescence microscopy images (Figure 10) the substrates sustain both cell adhesion and survival, confirming the biocompatibility of the material. Moreover, tubulin staining is positive only on one side of the scaffold (a), showing the presence of the cytoskeleton of human osteoblasts. Instead, on the opposite side, the tubulin staining is negative, and only the equine chondrocytes' nuclei have been counterstained (b).

Figure 8 Optical microscope image (5×) of the ME samples (8 layers) after four days of culture in static conditions

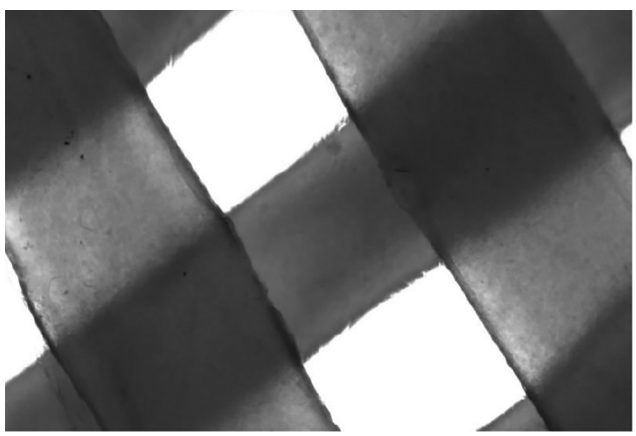

Figure 9 Optical microscope image (10×) of the hybrid samples after four days of culture in static conditions

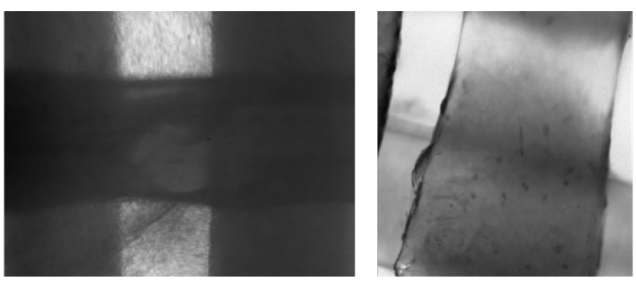

Figure 10 Fluorescent microscopy images of human primary osteoblasts (a, 20×) and equine primary chondrocytes (b, 10×) stained for Tubulin in green, and Hoechst in blue, seeded onto the two sides of substrate

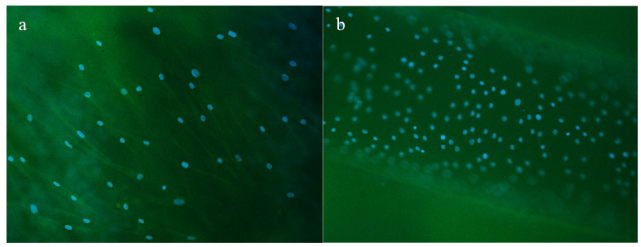

Discussion

This case study was focused on the production of multi-layered hybrid scaffolds consisting of ME and electrospun layers of the same polymer. The open source 3D printer Fab@home was used, mounting a grains extrusion head allowing strand formation and distribution on the plate according to the designed trajectory. Square grid samples were observed under optical microscope showing a good interconnectivity and spatial distribution of the pores. The electrospun mats were evaluated in terms of fibers diameter under SEM. The adhesion between the ME and ES layers was achieved by a DMA compression under specific thermo-loading conditions leading to a hybrid three-dimensional scaffold. The obtained hybrid scaffolds featured the different pore sides of the ME samples while the electrospun layers were produced with the same process parameters. The electrospun layers were mechanically evaluated under tensile loading-unloading tests. The mechanical response of the ME samples and the hybrid scaffolds was evaluated in compression tests, carried out at 23° C by means of the Instron 366 electromechanical analyzer. The hybrid scaffolds showed a peculiar mechanical response due to the presence of the ES layer put between the ME samples. The lower stiffness of the hybrid samples compared to the ME samples with the same total number of layers (8) can be interpreted on the basis of their modified morphology and structure. Moreover, the hybrid samples collapse is occurring at lower levels of stresses compared to the pure ME samples resulting in a softer material with tailored mechanical properties due to the final geometry of the hybrid structure. The different response of neat ME and hybrid scaffold can be ascribed to the thermomechanical history experience during layers adhesion of the latter system and to a consequent different bond between the layers. In fact, the cooling temperatures between the integration of electrospun fibers with ME layers have been demonstrated to play an important role on the mechanical properties of a hybrid scaffold made by two different polymers (Giannitelli *et al.*, 2015). Here, the same material has been used and the thermal adhesion between the differently processed layers influenced the mechanical

performances of the hybrid scaffolds. In particular, the hybrid structure showed only a partial melting of the electrospun fibers in correspondence to the ME filaments without a complete melting with respect to previous works using the same material (Giannitelli *et al.*, 2015; Liu *et al.*, 2007). Moreover, here the electrospun layers showed high porosity with a high degree of pores interconnection compared to the fibrous mats collected on the ME structures (Kim *et al.*, 2008). The biological characterization was carried out to allow a further comparison between the ME samples with 8 layers and the hybrid scaffolds. In particular, tests performed on the hybrid scaffolds were carried out by means of a static initial culture followed by a dynamic 3D culture in a bioreactor chamber while the ME samples were subjected only to the initial static culture test. A co-culture was chosen for the dynamic tests, thus human primary osteoblasts were seeded on one side of the scaffolds and equine primary chondrocytes on the other. The cellular colonization seemed to be highly promoted by the presence of the ES layer due to its surface morphology that promotes the cellular attachment and spreading on the entire hybrid structure. In this case, the population of the cells found on the filaments is strongly increased due to the containment effect caused by the ES layer. This containment has been observed through immunofluorescence analysis using an antibody specific for human tubulin not cross-reactive with the equine one. Tubulin staining was positive only on one side of the scaffold, showing the presence of the cytoskeleton of human osteoblasts. On the opposite side, instead, the tubulin staining was negative, and only the equine chondrocytes nuclei have been counterstained. The absence of tubulin positive osteoblasts on one side of the scaffold, shows how the ES layer kept the two different cell cultures separate, promoting their colonization only on their side.

Conclusions

The present work shows a new approach for the production of hybrid 3D scaffolds by using the same material without damaging the structures fabricated by two different technologies (ME and elettrospinning). The properties of the samples produced by each technology have been taken into account and used to produce a novel structure that can take advantage of surface, mechanical and chemical properties derived from the processing of the same material in two different ways. Moreover, the different structure of each layer is reported as an advantage for the formation of a proper interface tissue and not a barrier to the cellular migration during 3D culture tests. The future work will be oriented on the evaluation of the effects of the ME pores side on the cellular colonization and the co-culture proceeding. Moreover, the role of the produced hybrid scaffold on the formation of a complete osteochondral tissue will be evaluated as well as the capacity of the electrospun layer to promote the cellular attachment while providing the right support to the cellular phenotypes.

References

Agarwal, S., Wendorff, J.H. and Greiner, A. (2008), "Use of electrospinning technique for biomedical applications", *Polymer*, Vol. 49 No. 26, pp. 5603-5621.

Ahn, S.H., Lee, H.J., Bonassar, L.J. and Kim, G.H. (2012), "Cells (MC3T3-E1)-laden alginate scaffolds fabricated by a modified Solid-Freeform fabrication process supplemented with an aerosol spraying", *Biomacromolecules*, Vol. 13 No. 9, pp. 2997-3003.

Castells-Sala, C., Alemany-Ribes, M., Fernandez-Muiños, T., Recha-Sancho, L., López-Chicón, P., Aloy-Reverté, C., Caballero-Camino, J., Márquez-Gil, A. and Semino, C.E. (2013), "Current applications of tissue engineering in biomedicine", *Journal of Biochips & Tissue Chips*, S2:004, doi: 10.4172/2153-0777.S2-004.

Ceretti, E., Ginestra, P., Neto, P.I., Fiorentino, A. and Da Silva, J. (2017), "Multi-layered scaffolds production via fused deposition modeling (FDM) using an open source 3D printer: process parameters optimization for dimensional accuracy and design reproducibility", *Procedia Cirp*, Vol. 65, pp. 13-18.

Chen, R., Morsi, Y., Patel, S., Ke, Q.F. and Mo, X.M. (2009), "A novel approach via combination of electrospinning and FDM for tri-leaflet heart valve scaffold fabrication", *Frontiers of Materials Science in China*, Vol. 3 No. 4, pp. 359-366.

Dalton, P.D., Vaquette, C., Farrugia, B., Dargaville, T.R., Brown, T.D. and Hutmacher, D.W. (2013), "Electrospinning and additive manufacturing: converging technologies", *Biomaterials Science*, Vol. 1 No. 2, pp. 171-185.

Domingos, M., Dinucci, D., Cometa, S., Alderighi, M., Bartolo, P.J. and Chiellini, F. (2009), "Polycaprolactone scaffolds fabricated via bioextrusion for tissue engineering applications", *International Journal of Biomaterials*, Vol. 2009, p. 9, doi: 10.1155/2009/239643.

Ferraro, R.M., Ginestra, P.S., Lanzi, G., Giliani, S. and Ceretti, E. (2017), "Production of micro-patterned substrates to direct human iPSCs-derived neural stem cells orientation and interaction", *Procedia Cirp*, Vol. 65, pp. 225-230.

Gastaldi, D., Parisi, G., Lucchini, R., Bignozzi, S., Ginestra, P. S., Filardo, G., Contro, R., Kon, E. and Vena, P. (2015), "A predictive model for the elastic properties of a Collagen-hydroxyapatite porous scaffold for multi-layer osteochondral substitutes", *International Journal of Applied Mechanics*, Vol. 7 No. 4, p. 1550063.

Giannitelli, S.M., Mozetic, P., Trombetta, M. and Rainer, A. (2015), "Combined additive manufacturing approaches in tissue engineering", *Acta Biomaterialia*, Vol. 24, pp. 1-11.

Ginestra, P.S., Madou, M. and Ceretti, E. (2019), "Production of carbonized micro-patterns by photolithography and pyrolysis", *Precision Engineering*, Vol. 55, pp. 137-143.

Ginestra, P.S., Fiorentino, A. and Ceretti, E. (2017a), "Micro-structuring of titanium collectors by laser ablation technique: a novel approach to produce micro-patterned scaffolds for tissue engineering applications", *Procedia Cirp*, Vol. 65, pp. 19-24.

Ginestra, P.S., Ghazinejad, M., Madou, M. and Ceretti, E. (2016), "Fabrication and characterization of polycaprolactone-graphene powder electrospun nanofibers", Proceeding of SPIE 9932, Carbon Nanotubes, Graphene, and Emerging 2D Materials for Electronic and Photonic Devices IX, 99320A.

Ginestra, P.S., Pandini, S., Fiorentino, A., Benzoni, P., Dell'Era, P. and Ceretti, E. (2017b), "Microstructured

scaffold for cellular guided orientation: pCL electrospinning on laser ablated titanium collector", *CIRP Journal of Manufacturing Science and Technology*, Vol. 19, pp. 147-157.

Inverardi, N., Ginestra, P.S., Ferraro, R.M., Tonello, S., Marziano, M., Merlettini, A. and Gualandi, C (2018), "Shape memory electrospun nonwovens based on crosslinked poly(ϵ-caprolactone) for multifunctional biological applications", *Proceedings of AIP Conference*, Vol. 1981, 11 July, Article number 020006.

Kim, G.H., Son, J.G., Park, S.A. and Kim, W.D. (2008), "Hybrid process for fabricating 3D hierarchical scaffolds combining rapid prototyping and electrospinning", *Macromolecular Rapid Communications*, Vol. 29 No. 19, pp. 1577-1581.

Kundu, J., Shim, J.H., Jang, J., Kim, S.W. and Cho, D.W. (2015), "An additive manufacturing-based PCL-alginate-chondrocyte bioprinted scaffold for cartilage tissue engineering", *Journal of Tissue Engineering and Regenerative Medicine*, Vol. 9 No. 11, pp. 1286-1297.

Lara-Padilla, H., Mendoza-Buenrostro, C., Cardenas, D., Rodriguez-Garcia, A. and Rodriguez, C.A. (2017), "Influence of controlled cooling in bimodal scaffold fabrication using polymers with different melting temperatures", *Materials*, Vol. 10 No. 6, pp. 640.

Li, D., Yuliang, W. and Younan, X. (2003), "Electrospinning of polymeric and ceramic nanofibers as uniaxially aligned arrays", *Nano Letters*, Vol. 3 No. 8, pp. 1167-1171.

Li, D., Yuliang, W. and Younan, X. (2004), "Electrospinning nanofibers as uniaxially aligned arrays and layer-by-layer stacked films", *Advanced Materials*, Vol. 16 No. 4, pp. 361-366.

Liu, C., Xia, Z. and Czernuszka, J.T. (2007), "Design and development of three-dimensional scaffolds for tissue engineering", *Chemical Engineering Research and Design*, Vol. 85 No. 7, pp. 1051-1064.

Martins, A., Chung, S., Pedro, A., Sousa, R., Marques, A., Reis, R. and Neves, N. (2009), "Hierarchical starch-based fibrous scaffold for bone tissue engineering applications", *Journal of Tissue Engineering and Regenerative Medicine*, Vol. 3 No. 1, pp. 37-42.

Moroni, L., Schote, L.R., Hamann, D., de Wijn, J. and van Blitterswijk, C. (2008), "3D fiber-deposited electrospun integrated scaffolds enhance cartilage tissue formation", *Advanced Functional Materials*, Vol. 18 No. 1, pp. 53-60.

Mota, C., Puppi, D., Dinucci, D., Errico, C., Bártolo, P. and Chiellini, F. (2011), "Dual-scale polymeric constructs as scaffolds for tissue engineering", *Materials*, Vol. 4 No. 3, pp. 527-542.

Park, S.H., Kim, T.G., Kim, H.C., Yang, D.Y. and Park, T.G. (2008), "Development of dual scale scaffolds via direct polymer melt deposition and electrospinning for applications in tissue regeneration", *Acta Biomaterialia*, Vol. 4 No. 5, pp. 1198-1207.

Rasband, W.S. (2011), "US National institutes of health, bethesda, Maryland, USA, 1997-2014", available at: http://imagej.nih.gov/ij/

Sobral, J.M., Caridade, S.G., Sousa, R.A., Mano, J.F. and Reis, R.L. (2011), "Three-dimensional plotted scaffolds with controlled pore size gradients: effect of scaffold geometry on mechanical performance and cell seeding efficiency", *Acta Biomaterialia*, Vol. 7 No. 3, pp. 1009-1018.

Wei, C. and Dong, J. (2014), "Hybrid hierarchical fabrication of three-dimensional scaffolds", *Journal of Manufacturing Processes*, Vol. 16 No. 2, pp. 257-263.

Wunner, F.M., Wille, M.L., Noonan, T.G., Bas, O., Dalton, P.D., De-Juan-Pardo, E.M. and Hutmacher, D.W. (2018), "Melt electrospinning writing of highly ordered large volume scaffold architectures", *Advanced Materials*, Vol. 30 No. 20, p. 1706570.

Zein, I., Hutmacher, D.W., Tan, K.C. and Teoh, S.H. (2002), "Fused depositiong modeling of novel scaffold architectures for tissue engineering applications", *Biomaterials*, Vol. 23 No. 4, pp. 1169-1185.

Corresponding author

Paola Ginestra can be contacted at: paola.ginestra@unibs.it

For instructions on how to order reprints of this article, please visit our website:
www.emeraldgrouppublishing.com/licensing/reprints.htm
Or contact us for further details: **permissions@emeraldinsight.com**